Progress In Electromagnetics Research, Vol. 113, 67–82, 2011

IMPEDANCE MATCHING CAPABILITY OF NOVEL SOCKET CONTACTOR DESIGN USING VARIABLE OPEN STUBFOR RF PACKAGING TESTING

S.-M. Wu and K. Y. Wang

Department of Electrical Engineering
National University of Kaohsiung
No. 700, Kaohsiung University Road, Nan-Tzu District
Kaohsiung, Taiwan, R.O.C.

C.-H. Liu

JG Microtech Co. Ltd.
No. 16, Ln. 37, Sec. 2, Renhe Road, Daxi Township
Taoyuan County 335, Taiwan, R.O.C.

Abstract—In this paper, we will propose a new structure for a socket contactor applied to the lead-frame test board. This structure contains a variable open stub to match the impedance of the package and the load board. Its electrical property is considered superior to a conventional spring probe's, especially when it is applied to a QFP device. We will present its equivalent model and discuss this in detail. Note that the transmission line model we use is at this point a substitute for a physical structure. First, its RLC model will be constructed after we demonstrate its simulation and test data. Finally, we will use the MonteCarlo Method to analyze length inaccuracies in manufacturing and observe how this new structure works.

1. INTRODUCTION

An ever-increasing level of electrical and mechanical performance accuracy has become the most significant factor in socket and contactor technology in order to realize high-speed functioning beyond the GHz of a wafer or a package [1], since highly precise performance testing enables a designer to determine which design scheme may

Received 15 December 2010, Accepted 20 January 2011, Scheduled 27 January 2011
Corresponding author: Sung-Mao Wu (sungmao@nuk.edu.tw).

be properly applied. Numerous types of contact solutions have been developed [2–5]. One of the most popular technologies utilizes a spring probe as the contact medium between an IC lead frame and a PCB pad [6, 7]. However, this typical application has its disadvantages. For instance, its contact resistance determines the magnitude of the electric current that can flow through a particular contact [8]. If the resistance becomes higher than anticipated, it will be difficult for the electric current to pass through. Another problem lies in the lack of repeatability and reproducibility for a given measuring system. Repeatability and reproducibility measure different capabilities in a contactor: repeatability is the capacity of the same gauge to give consistent measurement readings no matter how many times the same operator of the gauge repeats the measurement process [9]. Reproducibility, on the other hand, is the ability of the same gauge to give consistent measurement readings regardless of who performs the measurements. A test result might also fluctuate every time due to the spring installed inside a spring probe. Furthermore, the bandwidth of a spring probe is too low to achieve high-frequency operation [10, 11].

The present new structure has several advantages. It has lower contact resistance due to its wider contact area. Its measured repeatability and reproducibility results are identical whenever gauged, since its shape is fixed. And its testing bandwidth is better than a spring probe's. Thus, we conclude that this particular structure is capable of ensuring impedance matching through modulation of its length.

We would like to use a QFP socket contactor to correct the defect in a spring probe's high-frequency performance. Since the major factor influencing the signal transmission of a socket contactor is impedance matching, we apply a single-stub impedance matching method to construct a new structure; it is apparently much easier to accomplish our goal of impedance matching by tuning the length of an opened stub. To verify that the advantages we have claimed above are correct, we also use simulation software to derive several formulas and analyze the contactor's electrical property. A transmission line structure from microwave engineering theory is used to equalize the contactors. The main purpose of its two terminals is to achieve impedance matching by modulating the length of the transmission line. Software can be used to verify the accuracy of the formulae. We will then compare the simulation results with the outcome of our formulae derivations and measured data.

2. PHYSICAL STRUCTURE AND MATCHING MODEL THEOREM

2.1. Physical Structure of Socket Contactor

This unique socket, newly designed for the purpose of testing a QFP package, is shown in Fig. 1. The major distinctions between it and a conventional socket with spring probes are its unusual contactors and its housing body, which is used to fix the contactors and ground pins (see Fig. 2). The ν-shaped contactor installed at the center of the apparatus is shown in Fig. 2(a). This was fastened to the housing with an open stub (at the right end of the contactor) when the tested package was pressed down. In other words, a QFP package was placed onto the center portion of the socket when testing began. Then the contactor's left end was pushed down by the lead frame, as illustrated in Fig. 2(a), and the load board was contacted at its turning point. As a result, the package and the load board were connected on the left side.

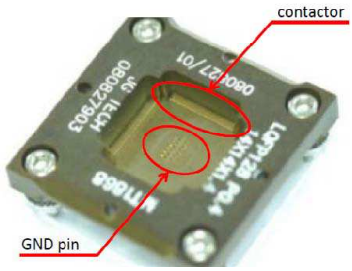

Figure 1. Novel socket of QFP package.

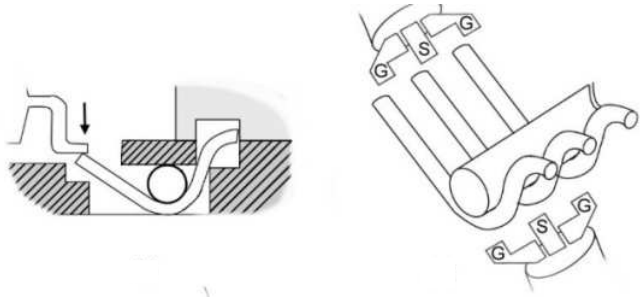

(a) (b)

Figure 2. Lateral view of socket contactor.

A 3D diagram demonstrating how the signal was transmitted is shown in Fig. 2(b). The signal was transmitted through the new device with a signal pin while the others were ground pins, as shown in Fig. 2(b). The housing is regarded as a material medium of the transmission line, since its relative dielectric constant (ε_r) can influence the performance of the entire socket. We can apply this typical structure to transmit a signal with a higher frequency, as it is similar to the CPW.

Consequently, in addition to its other merits, this special mechanism can fulfill the requirement of impedance matching by tuning along the length of its open stub. However, when a spring probe is used to perform an IC test, the total length of the spring probe shrinks whenever the package is pressed down. The major problem is that its shortened length is not always precisely identical. Furthermore, it usually accompanies potential fluctuation in the electrical property each time it is compressed. Hence, inconsistent test results are obtained. To correct this defect, the contactor is designed to be like a seesaw during testing. Every time it is pushed down, its turning point becomes a fulcrum. Since it alone makes the entire structure slant to the left, the contactor's length is unchanged and thus an identical electrical property can be ensured.

2.2. Matching Model Theorem

The crucial factor in ensuring an integral high-frequency signal from a signal generator to a load end is to maintain impedance matching during transmission. Indeed, whether or not the socket has actually met the requirements of impedance matching (between the output impedance of a package and the input impedance of a test load board) is not always taken into consideration since in the past a signal passing through a socket was not transmitted within the high-frequency range. Nevertheless, since the latest IC package's operating frequency has been incrementally increased, we can no longer ignore the effect of impedance matching. In contrast to a conventional spring probe, the contactor is considered a highly effective device for network impedance matching between the package and the load board.

Figure 2(b) presents a 3D view of the newly designed contactor and each type of signal transmission. The contactor is a two-port network: one end connects to the package as the output port (upper left corner) and the other connects to the load board as the input port (lower right corner). They then connect with the GSG (Ground, Signal, Ground) terminals; these three pins can be considered a typical CPW transmission line. We have therefore chosen the ideal transmission line to be an equivalent model of our contactor

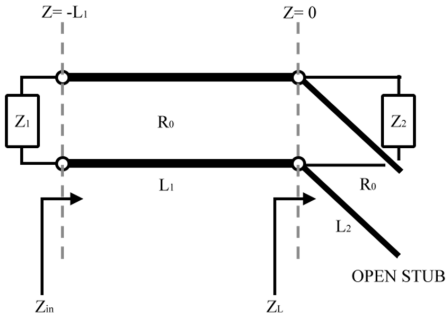

Figure 3. Equivalent transmission line model of socket contactor.

mechanism. The transmission line can be divided into two sections: a common transmission line connecting port #1 and port #2, and a single open stub connecting the transmission line and port #2, as shown in Fig. 3. The equivalent model is clearly similar to a single-stub shunt tuning circuit. Note that Z_1, specified below, stands for the output impedance of the package, and Z_2 represents the input impedance of the load board. The transmission line connecting port #1 and port #2 is on the left-hand side of the contactor in Fig. 2(a), while the open stub is situated on its right-hand side. The length of transmission line from port #1 to port #2 is L_1 and the length of the open stub is L_2. R_0 is the characteristic impedance of the transmission line (note that we use a lossless transmission line), which may be altered along with the socket medium and the contactor's spacing.

The contactor length can be tuned in two steps. First, we may change the length of it between the package and the load board. Given different package sizes, we might have to fix it by altering L_1 and the spacing. R_0 can be changed in accordance with the following spacing. If Z_1 and Z_2 are already given, L_1 and R_0 will remain steady along with the length and spacing of the contactor. Hence, the only parameter that can be tuned is L_2. Second, we can change the length of the open stub for impedance matching by using the single-stub shunt tuning method, which can minimize the effect of the contactor.

In the following, we show how to derive a formula for calculating the contactor's lengths (L_1, L_2), the impedances of the package and the load board (Z_1, Z_2), and the characteristic impedance, R_0. Based on this particular formula, we can determine the lengths of a contactor to match the impedance for a variety of projects. We separate the equivalent model from the point $Z = 0$ at the turning point of the contactor. Z_L is its input impedance measured from $Z = 0$. It connects

parallel with Z_2 and the open stub:

$$\frac{1}{Z_L} = \frac{1}{R_2 + jX_2} + \frac{1}{-jR_0 \cot \beta L_2} \tag{1}$$

Considered from the point $Z = 0$ via a transmission line to the point $Z = -L_1$, the input impedance will change to Z_{in}:

$$\Gamma(0) = \frac{Z_L - R_0}{Z_L + R_0} \tag{2}$$

$$\Gamma(Z = -L_1) = \Gamma(0)e^{-2j\beta L_1} = \frac{Z_{in} - Z_0}{Z_{in} + Z_0} \Rightarrow Z_{in} = R_0 \frac{Z_L + jR_0 \tan \beta L_1}{R_0 + jZ_L \tan \beta L_1} \tag{3}$$

To achieve the impedance matching requirement, Z_1 and Z_{in} must be conjugated, so Z_{in} is set as equal to Z_1, $Z_{in} = Z_1^*$. Hence, we can apply it to the following equations to obtain the open stub's length:

$$Z_L = R_L + jX_L \tag{4}$$

$$Z_{in} = R_1 - jX_1 = \frac{R_0(R_L + jX_L) + jR_0^2 \tan \beta L_1}{R_0 + j(R_L + jX_L) \tan \beta L_1}$$

$$= \frac{R_0 R_L + j\left(R_0 X_L + R_0^2 \tan \beta L_1\right)}{(R_0 - X_L \tan \beta L_1) + j(R_L \tan \beta L_1)} \tag{5}$$

$$\Rightarrow \begin{cases} (X_1 \tan \beta L_1 - R_0)R_L - (R_1 \tan \beta L_1)X_L = -R_0 R_1 \\ (R_1 \tan \beta L_1)R_L + (X_1 \tan \beta L_1 - R_0)X_L = R_0(X_1 + R_0 \tan \beta L_1) \end{cases} \tag{6}$$

To simplify the above, let $A = X_1 \tan \beta L_1 - R_0$ and $B = R_1 \tan \beta L_1$

$$\Rightarrow AR_L - BX_L = -R_0 R_1 \tag{7}$$

$$BR_L + AX_L = R_0(X_1 + R_0 \tan \beta L_1) \tag{8}$$

Let (7) $\times B -$ (6) $\times A \Rightarrow R_L$ and (7) $\times A -$ (6) $\times B \Rightarrow X_L$

$$\Rightarrow R_L = \frac{R_0\left[2R_1 X_1 \tan \beta L_1 + R_0 R_1\left(\tan^2 \beta L_1 - 1\right)\right]}{(R_1^2 - X_1^2)\tan^2 \beta L_1 + R_0(2X_1 \tan \beta L_1 - R_0)} \tag{9}$$

$$\Rightarrow X_L = \frac{R_0\left[\left(R_1^2 + X_1^2 - R_0^2\right)\tan \beta L_1 + R_0 X_1\left(\tan^2 \beta L_1 - 1\right)\right]}{\left(R_1^2 - X_1^2\right)\tan^2 \beta L_1 + R_0\left(2X_1 \tan \beta L_1 - R_0\right)} \tag{10}$$

Examining the results of Equations (9) and (10) reveals that a relationship between the package (Z_1), the transmission line (L_1), and the load impedance ($Z_L = R_L + jX_L$) has been established. Furthermore, the load impedance is shunted by using the open stub (L_2) and the load board (Z_2). To fulfill its input impedance matching

requirement $Z_{in} = Z_1^*$, the open stub's length has to be tuned to match the load impedance, as shown in Equations (9) and (10).

$$\frac{1}{Z_L} = \frac{1}{R_2 + jX_2} + \frac{1}{-jR_0 \cot \beta L_2} \tag{11}$$

$$Z_L = \frac{R_0^2 R_2 - j\left[R_0\left(R_2^2 + X_2^2\right)\tan \beta L_2 - R_0^2 X_2\right]}{R_0^2 + \tan^2 \beta L_2 - 2R_0 X_2 \tan \beta L_2} \tag{12}$$

Equation (12) suggests a relationship between the load impedance, the open stub, and the load board. The load impedance is identical to Equations (9), (10), and (12). That is: (12) = (9) + j(10)

From the real part:

$$\frac{R_0 R_2}{R_0^2 + \tan^2 \beta L_2 - 2R_0 X_2 \tan \beta L_2} = \frac{2R_1 X_1 \tan \beta L_1 + R_0 R_1\left(\tan^2 \beta L_1 - 1\right)}{\left(R_1^2 - X_1^2\right)\tan^2 \beta L_1 + R_0\left(2X_1 \tan \beta L_1 - R_0\right)} \tag{13}$$

From the imaginary part:

$$\frac{-\left(R_2^2 + X_2^2\right)\tan \beta L_2 + R_0 X_2}{R_0^2 + \tan^2 \beta L_2 - 2R_0 X_2 \tan \beta L_2} = \frac{\left(R_1^2 + X_1^2 - R_0^2\right)\tan \beta L_1 + R_0 R X_1\left(\tan^2 \beta L_1 - 1\right)}{\left(R_1^2 - X_1\right)\tan^2 \beta L_1 + R_0\left(2X_1 \tan \beta L_1 - R_0\right)} \tag{14}$$

The formulae above can help us determine the contactor's length. As we know, the output impedance of a certain package and a load board's impedance are given at the design stage. Once we settle the package size and the spacing between contactors, the characteristic impedance will be constant accordingly. The propagation constant of the transmission line, β, depends on the operating frequency of the impedance matching. The unknown variables L_1 and L_2 can be solved using Equations (13) and (14).

In short, we try first to acquire a valid calculation of the contactor's length, and then we can determine the impedance matching between the package and the load board. For example, assume that $Z_1 = R_1 = 40\,\Omega$, $Z_2 = R_2 = 60\,\Omega$ and $R = 50\,\Omega$. This implies that $X_1 = X_2 = 0$. Therefore, Equations (13) and (14) can be simplified to (15); this new formula then changes into a relationship between L_1 and L_2. If we assign a certain value to L_1, L_2 will be solved using Equation (15).

$$\tan^2 \beta L_2 = \frac{R_1\left(R_1 R_2 - R_0^2\right)\tan^2 \beta L_1 + R_0^2(R_1 - R_2)}{R_1(\tan^2 \beta L_1 - 1)} \tag{15}$$

Assume $L_1 = 0.4\lambda$, $\beta = \frac{2\pi}{\lambda}$, and $L_2 = 0.247\lambda$. At 2.4 GHz, $L_1 = 56$ mm and $L_2 = 33.7$ mm.

With the given variables and according to Equation (15), we can decide on the best length ratio for our contactor. To achieve impedance matching at $L_1 = 0.4\lambda$, the open stub needs to be tuned to 0.247λ. If we transmit a 2.4 GHz signal, the physical lengths of L_1 and L_2 are set at $L_1 = 56$ mm and $L_2 = 33.7$ mm. Our simulation results are illustrated in Figs. 4(a) and (b). S_{21} is close to zero at 2.4 GHz, implying that transmission can be kept in a $1:1$ unity gain, minimizing signal loss when passing across the socket. The formula established for the equivalent model can help us estimate the performance of this newly created structure (Fig. 4).

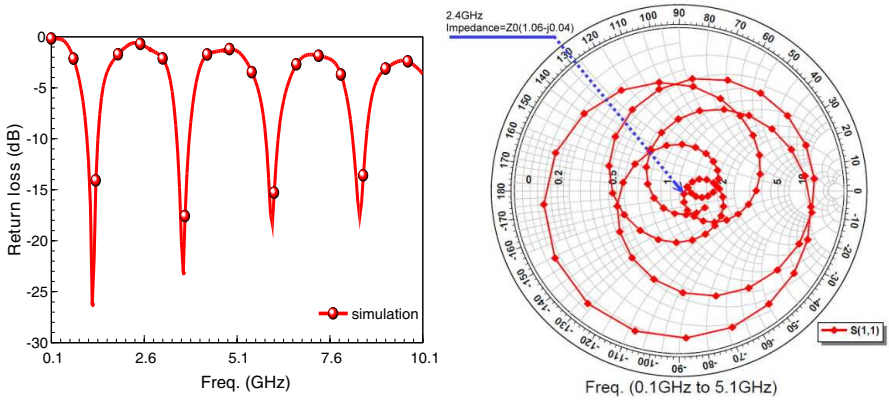

Figure 4. (a) Return loss for the derived formula. (b) Input impedance match on Smith chart.

To apply Equation (14), we need to fix two variables in advance: the length of the transmission line (L_1) and the operating frequency. Since the contactor is slanted, the socket's height will be determined by the length of the transmission line. The length of the open stub depends on the different operating frequencies. In the following, we demostrate a 3D electromagnetic (EM) simulation of an actual structure. Then we compare our formula, the EM simulation, and the measured data.

3. SIMULATION AND MEASUREMENT

Figure 5 presents a 3D model of our unique socket contactor. First we suppose that a given length of transmission line is 0.6 mm, so the length of single-stub tuning would be 0.4 mm. Then, three contactor pins are installed in parallel, similar to a coplanar waveguide. Next, we substitute the length parameter into the formula to simulate an equivalent transmission line model. After that, a 3D physical model (Fig. 5) is imported into the 3D EM simulation software. Finally, we compare the measured results with those from these two simulation methods.

The S-parameter data from the two simulation methods is shown in Fig. 6. According to impedance matching theory in microwave engineering, the value of the return loss will be less than -20 dB and

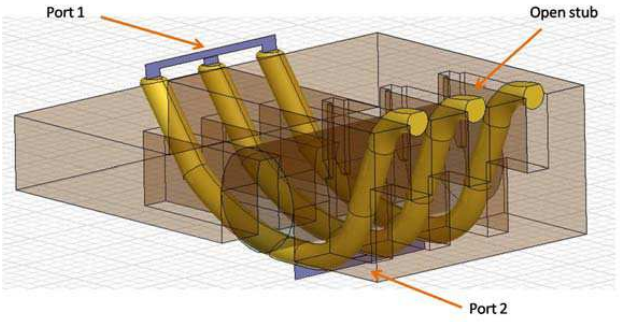

Figure 5. 3D diagram of socket contactor.

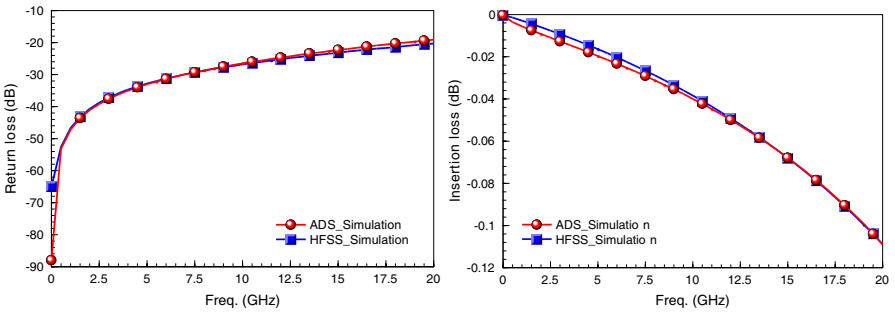

Figure 6. (a) Return loss for contactor simulation result. (b) Insertion loss for contactor simulation result.

the value of the insertion loss will be approximately 0 dB. Compared with these two simulation results, we can see that the return loss is very approximate, and both values are less than −20 dB from 0.1 GHz to 20 GHz, as shown in Fig. 6(a). The insertion loss for both simulation methods is 0 dB. Although the actual results compared with the two simulations are not the same, the values are very close.

Having established the accuracy of the equivalent model using a single stub, we wish to verify that the relevant formula can represent the difference between impedance matching and non-matching. We fix the length of the open stub, then extend the length between Port #1 and Port #2. Now, we can compare the different lengths to once again verify the formula. The simulation results are displayed in Figs. 7(a) and (b), with 7(a) showing the return loss (S11) for the different lengths between Port 1 and Port 2, and 7(b) showing the insertion loss (S21). In the figure, S11_1 indicates that we extended the length to 1 mm, S11_1_4 to 1.4 mm, and S11_7 to 1.7 mm.

Comparing Figs. 7(a) and (b), we see that the return loss (S11) at 18 GHz is −20 dB for impedance matching, but the −20 dB trace point S11_1 is only 2GHz, while trace S11_1_4 and trace S11_1_7 are worse than S11_1.

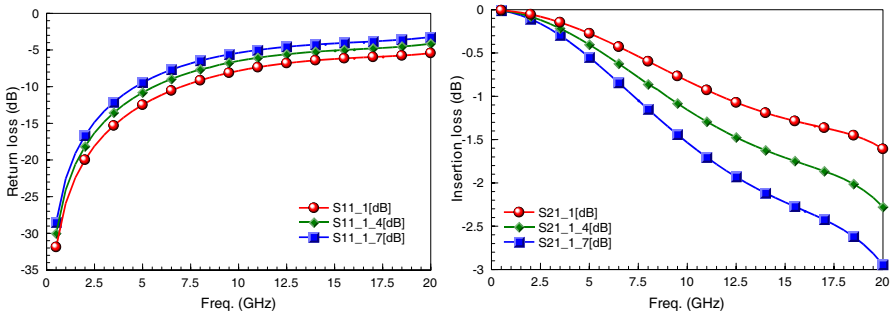

(a) (b)

Figure 7. (a) Return loss for different contactor lengths in simulation result. (b) Insertion loss for different contactor lengths in simulation result.

Given the above simulation results, the influence of impedance matching on the socket contactor cannot be neglected. As the following figures show, the measured data and simulation results display the same trend. The socket contactor measurement data has been under de-embedded. Due to a processing problem, our measured contactor impedance did not match at the operating frequency. The return loss is −20 dB at 10 GHz and −10 dB at 15 GHz.

Figure 8(a) presents the measurement set-up and Fig. 8(b) a schematic diagram of the same. To measure the novel contactor we used two test fixtures and placed the socket in the middle of them. First we measured the test fixtures only (probe lands on trace's two sides), then we obtained the whole socket measurement data (combined with the contactor and test fixtures). In this way, the contactor's real effect could be extracted using de-embedding method [12–14]. The measurement data and simulation are presented in Fig. 9. The measurement data include via, contactor, and the trace on the bottom test fixture; we used de-embedding method to remove the effect of the via and trace. Comparison with the simulation results and measurement data indicates that the two traces are closed, which means the formulae are useful and accurate for designing this novel structure.

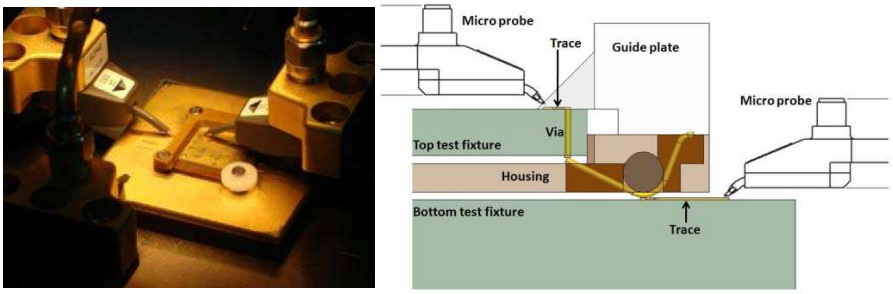

Figure 8. (a) Measurement set-up with fixture. (b) Lateral view diagram of measurement set-up.

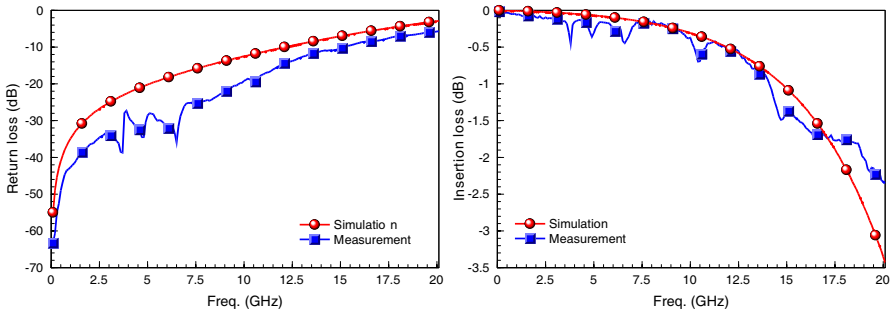

Figure 9. (a) Return loss for contactor measurement result. (b) Insertion loss for contactor measurement result.

4. MODEL EXTRACTING AND MONTE CARLO ANALYSIS

4.1. Model Extracting

According to the above results, electrical and mechanical performance should be considered along with circuit design. The SPICE model was used for co-design with the package and load board [15]. By comparing the simulation results from the equivalent model and the measurement data, we can verify that the method using our formula is credible. In the previous section, "Matching Model Theorem", we chose the transmission line as the equivalent model and derived the formula for impedance matching. In this section we present the SPICE model [16–18], the physical structure of which is shown in Fig. 10 while the SPICE model list is given in Table 1.

The model is divided into two parts — signal transmission terminal and open stub — and has four elements on the signal

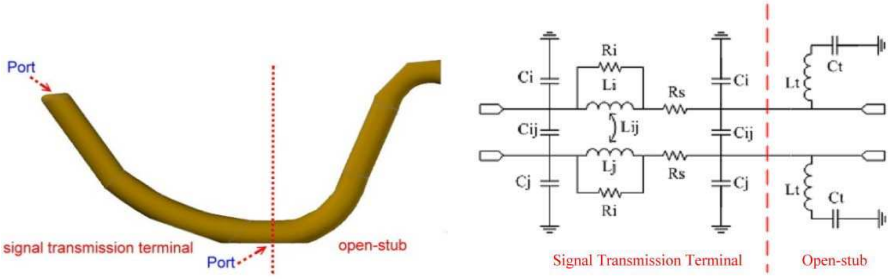

Figure 10. (a) Lateral view of socket contactor. (b) SPICE model of socket contactor.

Table 1. SPICE model list of socket contactor.

C_{ij}	Mutual Capacitance	0.025 fF
C_i, C_j	Shunt Capacitance	0.082 pF
L_{ij}	Mutual Inductance	0.56 nH
L_i, L_j	Loop Inductance	1.4 nH
L_t	Series Inductance of Transmission Line Model	0.05 nH
C_t	Shunt Capacitance of Transmission Line Model	0.8 pF
R_i	Rskin(High-Frequency Loss)	10k ohm
R_s	Series Resistance	0.35 ohm

transmission terminal: L_i and L_j are the inductance on the traces, with i and j indicating traces 1 and 2; C_i and C_j are the capacitance between trace and ground; R_s is the series resistance through the trace; and in consideration of the high-frequency skin effect, R_i represent the high-frequency loss. In addition to the four elements on the traces, two elements represent the coupling effect between the two traces: C_{ij} and L_{ij} are mutual capacitance and inductance, respectively.

The SPICE model for the open stub is simple to express. L_t is the inductance on a trace and C_t is the capacitance caused by the opened. The value of each element is listed in Table 1.

4.2. Monte Carlo Analysis

The simulation results, measurement data, and SPICE model have been presented in Fig. 10. However, deviation will occur during the manufacturing process. To deal with this problem, the Monte Carlo analysis method was used to check impedance matching deviation. We assume two variables, L_1 and L_2, will be inexact during the manufacturing process. The novel contactor (shown in Fig. 11) is 1.7 mm long, including the transmission part and the open stub. The simulation results for the different lengths are presented in Fig. 12.

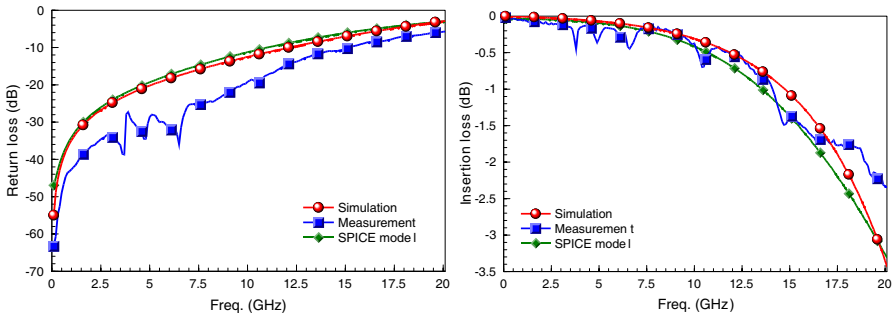

(a) (b)

Figure 11. (a) Return loss for contactor SPICE model result. (b) Insertion loss for contactor SPICE model result.

Comparison with Fig. 6 and Fig. 9 is instructive. Theoretically, the best design for impedance matching is able to reach −20 dB at 20 GHz (as shown in Fig. 6). But taking into consideration a processing problem, the first version of the design does not satisfy impedance matching at the operating frequency. Its impedance (with the magnitude of impedance $\sqrt{R^2 + X^2}$) is close to 50 at 9.4 GHz. So, we tune the lengths of L_1 and L_2 at this frequency.

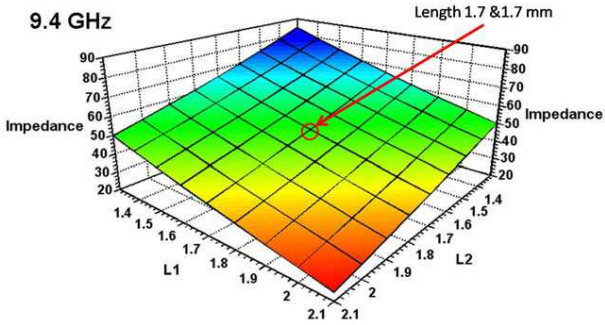

Figure 12. Monte Carlo analysis result for input impedance.

Assuming that variability in the manufacturing process is 5%, the length will vary between 1.6 mm and 1.8 mm, and the impedance will range from 60 to 40. As Fig. 12 indicates, the effect of such variability cannot be ignored. Improving the manufacturing process is another problem relevant to this novel structure, but we will not address that here.

5. CONCLUSION

Energy loss occurs on any structure when a high-frequency signal passes through it. How to restrain energy loss on trace let signal transmits integrality to the load end. This has become a popular and important issue in circuit design, one that also occurs in socket design. In this paper we have proposed impedance matching as the solution. In the "Simulation and Measurement" section we presented the performance of a novel contactor structure (Fig. 9). By comparing formulae, simulation data, and measurement data, we verified the accuracy of our equations. We also ensured the feasibility of using a transmission line as an equivalent model. Using analytical results it is easy to determine differences in performance before and after the design. The effect of impedance matching is clear, and our novel socket contactor structure solves the problem using impedance matching. The formulae in this paper provide the design guidelines for this novel structure.

In the future, this novel structure will be applicable not only for transmitting a single end type but also for differential and common mode signals. How does the performance representing under this situation. To increase this structure's accuracy, a novel 3D direct measurement method can be used without the effect of via on test fixture [19, 20]. This topic is worthy of further study.

REFERENCES

1. Hsu, H.-S. and H.-T. Hsu, "System level integration of simulation methods for high data-rate transmission circuit design applications," *Progress In Electromagnetics Research*, Vol. 90, 31–49, 2009.
2. Chandrasekar, K., J. Wilson, E. Erickson, Z. Feng, J. Xu, S. Mick, and P. Franzon, "Inductively coupled connectors and sockets for multi-Gb/s pulse signaling," *IEEE Transactions on Advanced Packaging*, Vol. 31, No. 4, 749–758, 2008.
3. Monti, G., R. de Paolis, and L. Tarricone, "Design of a 3-state reconfigurable CRLH transmission line bases on MEMS switches," *Progress In Electromagnetics Research*, Vol. 95, 283–297, 2009.
4. LaMeres, B. J., C. McIntosh, and M. Abusultan, "Novel 3-D coaxial interconnect system for use in system-in-package applications," *IEEE Transactions on Advanced Packaging*, Vol. 33, No. 1, 37–47, 2010.
5. Male, F., J. Lucas, and Y. Huan, "The experimental results of a low power X-band free electron maser by electron pre-bunching," *Progress In Electromagnetics Research*, Vol. 101, 43–62, 2010.
6. Barnes, H., J. Moreira, H. Ossoinig, M. Wollitzer, T. Schmid, and T. Ming, "Development of a pogo pin assembly and via design for multi-gigabit interfaces on automated test equipment," *IEEE Asia-Pacific Microwave Conference*, 2006.
7. Szendrenyi, B. B., H. Barnes, J. Moreira, M. Wollitzer, T. Schmid, and T. Ming, "Addressing the broadband crosstalk challenges of pogo pin type interfaces for high-density high-speed digital applications," *IEEE/MTT-S International Microwave Symposium*, 2007.
8. Sun, R.-B., R.-B. Wu, and S.-W. Hsiao, "Compromised impedance match design for signal integrity of pogo pins structures with different signal-ground patterns," *IEEE Workshop on Signal Propagation on Interconnects*, 2009.
9. Gessel, D., A. Slcoum, A. Sprunt, and S. Ziegenhagen, "Realistic spring probe testing methods and results," *IEEE Proceedings, International Test Conference*, 2002.
10. Andes, J. and E. Bogatin, "The socket response to current packaging and test trends," *IEEE/CPMT/SEMI 29th International*, 2004.
11. Sun, R.-B., C.-Y. Wen, Y.-C. Chang, and R.-B. Wu, "A new isolation structure for crosstalk reduction of pogo pins in a test socket," *IEEE Electrical Performance of Electronic Packaging and*

Systems, EPEPS 18th Conference, 2009.

12. Reynoso-Hernandez, J. A. and I.-G., Everardo, "A straightforward de-embedding method for devices embedded in test fixtures," *57th ARFTG Conference Digest — Spring*, 2001.
13. Zuniga-Juarez, J. E., J. A. Reynoso-Hernandez, and J. R. Loo-Yau, "Two-tier L-L De-embedding method for S-parameters measurements of devices mounted in test fixture," *Microwave Measurement Conference, 73rd ARFTG*, 2009.
14. Zhang, J., M. Y. Koledintseva, G. Antonini, J. L. Drewniak, A. Orlandi, and K. N. Rozanov, "Planar transmission line method for characterization of printed circuit board dielectrics," *Progress In Electromagnetics Research*, Vol. 102, 267–286, 2010.
15. Kung, F. W. L. and H. T. Chuah, "System modeling of high-speed digital printed circuit board using SPICE," *Progress In Electromagnetics Research*, Vol. 20, 179–211, 1998.
16. Wang, C.-C., C.-W. Kuo, S.-M. Wu, and H.-H. Cheng, "A novel time-domain approach for extracting broadband models of power delivery networks with resonance effect," *IEEE Transactions on Advanced Packaging*, Vol. 32, No. 3, 636–643, 2009.
17. Kungand, F. W. L. and H. T. Chua, "System modeling of high-speed digital printed circuit board using SPICE," *Progress In Electromagnetics Research*, Vol. 20, 179–211, 1998.
18. Mantysalo, M. and E. O. Ristolainen, "Modeling and analyzing vertical interconnections," *IEEE Transactions on Advanced Packaging*, Vol. 29, No. 2, 335–342, 2006.
19. Wu, S.-M. and S.-W. Guan, "A novel signal integrity methodology by 3D direct analysis for microwave testing probes," *Progress In Electromagnetics Research C*, Vol. 15, 187–199, 2010.
20. Zhen, Z. and K. L. Melde, "Development of a broadband coplanar waveguide-to-microstrip transition with vias," *IEEE Transactions on Advanced Packaging*, Vol. 31, No. 4, 861–872, 2008.